Published in final edited form as:
J Dermatol Sci. 2011 September ; 63(3): 164–172. doi:10.1016/j.jdermsci.2011.06.001.

L-3-Phosphoserine Phosphatase (PSPH) Regulates Cutaneous Squamous Cell Carcinoma Proliferation Independent of L-serine Biosynthesis

Michael A. Bachelor[1], **Yan Lu**[1], and **David M. Owens**[1,2,†]

[1] Department of Dermatology, Columbia University, College of Physicians and Surgeons, New York, NY 10032, USA

[2] Department of Pathology, Columbia University, College of Physicians and Surgeons, New York, NY 10032, USA

Abstract

Background—L-3-phosphoserine phosphatase (Psph) is a highly conserved and widely expressed member of the haloacid dehalogenase superfamily and the rate-limiting enzyme in L-serine biosynthesis. We previously found Psph expression to be uniquely upregulated in a α6β4 integrin transgenic mouse model that is predisposed to epidermal hyperproliferation and squamous cell carcinoma (SCC) formation implicating a role for Psph in epidermal homeostasis.

Objective—We examined the status of PSPH in normal skin epidermis and skin tumors along with its sub-cellular localization in epidermal keratinocytes and its requirement for squamous cell carcinoma (SCC) proliferation.

Methods—First, an immunohistochemical study was performed for PSPH in normal skin and skin cancer specimens and in cultured keratinocytes. Next, biochemical analyses were performed to confirm localization of PSPH and to identify candidate binding proteins. Finally, proliferation and apoptosis studies were performed in human SCC and normal keratinocytes, respectively, transduced with vectors encoding small hairpin RNAs targeting PSPH or overexpressing a phosphatase-deficient PSPH mutant.

Results—PSPH is expressed throughout the proliferative layer of the epidermis and hair follicles in rodent and human skin and is highly induced in SCC. In keratinocytes, PSPH is a cytoplasmic protein that primarily localizes to endosomes and is present primarily as a homodimer. Knock down of PSPH dramatically diminished SCC cell proliferation and cyclin D1 levels in the presence of exogenous of L-serine production suggesting a non-canonical role for PSPH in epithelial carcinogenesis.

Conclusions—Psph is highly induced in proliferative normal keratinocytes and in skin tumors. PSPH appears to be critical for the proliferation of SCC cells; however, this phenomenon may not involve the phosphoserine metabolic pathway.

[†]Correspondence: David M. Owens, Department of Dermatology, Columbia University, 1150 St. Nicholas Avenue, Room 312A, New York, NY 10032, USA, do2112@columbia.edu, Phone: 212-851-4544, Fax: 212-851-4810.

Conflict of interest

The authors report no conflict of interest.

Keywords

PSPH; epidermis; squamous cell carcinoma; keratinocyte; serine metabolism

1. Introduction

L-3-phosphoserine phosphatase (PSPH) is a member of haloacid dehalogenase (HAD) superfamily and contains a N-terminal DXDXT(T/V) motif, which is utilized to convert phospho-L-serine to L-serine [1–5]. As a precursor for the biosynthesis of diverse compounds including amino acids, neurotransmitters, phospholipids, glycolipids, purines, and thymidine, L-serine is linked to multiple fundamental aspects of cell behavior such as proliferation and differentiation in most tissues. Multiple lines of evidence in both experimental mouse models and patients suffering from congenital neurological abnormalities indicate that insufficient L-serine biosynthesis primarily impacts the development and proper functioning of the central nervous system [6–7]. On the other hand, augmented L-serine biosynthesis is associated with a number of cancer types in humans. For example, metastatic breast cancer features increased production of L-serine, which is thought to be critical for the proliferation of these metastatic cells, and correlates with poor prognosis in patients with bone metastases [8]. The role of PSPH in providing amino acid and nucleotide precursors to facilitate cell proliferation has been well documented and, accordingly, augmented PSPH levels have been observed in a number of human tumor types in including non-small-cell lung cancer [9], mesothelioma [10], metastatic breast [8] and gastric cancers [11], and pediatric brain tumors [12]. However, the functional significance of PSPH dysregulation in these tumors remains unclear.

We previously identified augmented levels of Psph in a α6β4 integrin transgenic mouse model that is predisposed to epidermal hyperproliferation and SCC formation [13] implicating a novel function for Psph in epidermal homeostasis. However, the status of PSPH in the skin and its potential role in maintaining epidermal homeostasis and skin carcinogenesis has been largely unexplored up to this point. Here, we provide evidence that PSPH is strongly expressed in proliferative keratinocytes in murine and human skin. In epidermal keratinocytes, PSPH is primarily present as a homodimer and is localized to endosomes organelles. PSPH is highly induced in murine and human SCC and knock down of PSPH expression abrogates SCC keratinocyte proliferation independent of L-serine levels.

2. Materials and Methods

2.1 Skin and skin tumor harvesting

De-identified human foreskin specimens were obtained through the services of the Skin Disease Research Center in the Department of Dermatology at Columbia University under IRB approval. Human cutaneous SCCs were collected from the Department of Dermatology at Columbia University Medical Center as previously described [14]. Dorsal murine skin specimens were surgically excised from eight-week old female FVB mice (Taconic). For immunolabeling studies, specimens were embedded in O.C.T. medium and cryopreserved or fixed in 10% formalin and paraffin-embedded. For RT-PCR studies, mice were shaved on the dorsal surface and 24 hours later received a single topical application of 5 nmol 12-*O*-tetradecanoylphorbol-13-acetate (TPA) (LC Laboratories) in 200 μl acetone or 200 μl acetone vehicle alone. Dorsal skins were surgically excised 4 hours following TPA and acetone treatment and flash frozen in liquid nitrogen. Murine skin papillomas and SCCs utilized in this study were induced in FVB mice using a standard two-stage chemical carcinogenesis protocol [14].

2.2 RT-PCR analysis

Total RNA was isolated from acetone- and TPA-treated Wt and α6β4 transgenic mouse skin epidermis and used to synthesize cDNA as previously described [15]. For semi-quantitative RT-PCR analysis cDNA samples were subjected to PCR analysis using 2X PCR Master Mix as per manufacturer instructions (Promega). Oligonucleotide primer pairs were designed to target separate exons in Psph (sense: 5′-ATGGTCTCCCACTCAGAGCTG-3′; anti-sense: 5′-ACAATGCTCCGAAAGCCACC-3′) and Gapdh (sense: 5′-AGTATGATGACATCAAGAAGG-3′; anti-sense: 5′-ATGGTATTCAAGAGAGTAGGG-3′) for each sample. PCR products were quantified by densitometry using NIH ImageJ software. For each sample, Psph levels were normalized by expression of Gapdh (n = 3 mice per group). Average Psph levels were statistically compared between acetone-treated Wt versus α6β4 transgenic mice ($p < 0.05$) and TPA-treated Wt versus α6β4 transgenic mice ($p < 0.05$) using a Student's t-Test.

2.3 Tissue culture

Primary normal mouse keratinocyte cultures were established in complete FAD medium as previously described [13–15]. Primary cultures of human normal and SCC keratinocytes were established in complete FAD medium as previously described [16]. For confluency studies, human SCC keratinocyte cultures huSCC13 and huSCC35 were counted using a Countess automated cell counter (Invitrogen) and seeded at equal density (10^5 cells/plate). After which, cultures were harvested on sequential days of growth between 20%, 40%, 80% and 100% confluency. HEK293 (kindly provided by Dr. David Bickers) and 293T packaging cells (kindly provided by Dr. Angela Christiano) were cultured in DMEM (Invitrogen) supplemented with 10% FBS (HyClone).

2.3.1 Retroviral transduction—Full-length Wt or phosphatase-deficient mutant ($Psph^{Asn20}$, please see Mutagenesis section below) murine Psph cDNA (Invitrogen) was tagged with EGFP using the pEGFP-N1 vector (Clontech) and subsequently subcloned into the pBabe retroviral vector [17]. In addition, EGFP cDNA alone was subcloned into pBabe as a control vector. Either pBabe empty (EV), pBabe-EGFP, pBabe-Psph-EGFP, pBabe-$Psph^{Asn20}$-EGFP vectors were transduced into normal murine keratinocytes using a dual packaging cell system as previously described [15–18].

2.3.2 Psph shRNA knock down—To ablate PSPH expression in huSCC cells, the pTRIPZ (Open Biosystems) a lentiviral vector encoding a short hairpin RNA against murine PSPH (pTRIPZ-PSPH, clone V2HS_47583, Open Biosystems) or control (pTRIPZ-NS) was utilized along with psPAX2 (Addgene 12260) and pMD2.G (Addgene 12259) plasmids to produce lentivirus to subsequently transduce huSCC cells as previously described [14]. Transduced huSCC cells were selected in 2 μg/mL puromycin (Sigma). PSPH knockdown was induced by treating transduced cells with 1 μg/ml Doxycycline (Dox) (Fisher Scientific) for 1–6 days.

2.3.3 Clonogenic assays—To measure proliferation, pTRIPZ-NS or pTRIPZ-PSPH huSCC13 and huSCC35 cells were plated at 2,000 cells/well as previously described [14–15] supplemented with 1 μg/ml Dox. Cultures were incubated for two weeks after which the 3T3 cells were removed and keratinocyte colonies were fixed and stained with Rhodamine. Total colonies > 4 mm in size were counted using NIH ImageJ software. Each time point was counted in triplicate for each group and average colony numbers were statistically compared using a Student's t-Test ($p < 0.05$) between pTRIPZ-NS or pTRIPZ-PSPH groups for each huSCC primary culture.

2.4 Generation and Purification of Psph Monoclonal Antibodies

Full-length recombinant murine Psph was tagged with glutathione *S*-transferase using the bacterial expression vector pETGEXCT vector and utilized to immunize mice to produce hybridomas generating monoclonal antibodies against Psph (A&G Pharmaceutical). 5 hybridoma clones were identified to specifically recognize Psph by immunoblot analysis using unpurified supernatant (data not shown). For all studies herein, clone 5B2 was chosen due to its relative high affinity and recognition of murine and human PSPH proteins. To harvest antibodies, 5B2 cell supernatants were purified using a Nunc ProPur™ Protein Purification Kit as per manufacturer instruction(Fisher Scientific).

2.5 Immunoblot analysis

Cultured cells were lysed in RIPA buffer containing 1 mM Na_3VO_4 (Sigma), 1mM phenylmethanesulphonylfluoride (PMSF) (Sigma), 1 μg/ml leupeptin (Sigma) and 1 μg/ml aprotinin (Sigma). Murine liver, brain and lung tissues were lysed in 10 mM Na_3PO_4 (Sigma), 1% Triton (Sigma), 1% SDS (Fisher Scientific), 150 mM NaCl (Fisher Scientific), 0.5% sodium deoxycholate, 1mM PMSF, 1 μg/ml leupeptin and 1 μg/ml aprotinin. Human liver and lung nuclear lysates were purchased from Active Motif. 10–20 μg of protein were subjected to SDS-PAGE on Novex Tris-Glycine Gels (Invitrogen), and transferred proteins were probed with the following primary antibodies: Psph (5B2), β-actin (Cell Signaling), GFP (AbCam), cleaved PARP (Cell Signaling), β-tubulin (Sigma), cyclin D1 (Santa Cruz) or Rb (Cell Signaling). Primary antibodies were detected with species-specific horseradish peroxidase-conjugated secondary antibodies (Jackson ImmunoResearch) followed by ECL (GE Healthcare Life Sciences).

2.6 Immunoprecipitation studies

For tandem affinity purification analysis, full-length murine Psph cDNA (Invitrogen) was N-terminal tagged with HA and C-terminal tagged with FLAG and sub-cloned into the pcDNA3.1 expression vector (Invitrogen). HA-Psph-FLAG-pcDNA3.1 or empty pcDNA3.1 was transfected into HEK293 cells using Lipofectamine as per manufacturer instruction (Invitrogen). Transfected cells were lysed in buffer containing 50 mM Tris-HCl, 150 mM NaCl, 1 mM EDTA, 1% NP40 (US Biological), 1mM PMSF, 1 μg/ml leupeptin and 1 μg/ml aprotinin and incubated with α-FLAG-conjugated sepharose beads (Sigma) followed by competitive elution with the FLAG peptide (Sigma). Next, lysates were incubated with α-HA-conjugated sepharose beads followed by competitive elution with HA peptide (Roche). Eluants were subjected to SDS-PAGE after which gels were stained using the SilverSNAP Stain for Mass Spectrometry kit as per manufacturer instruction (Pierce) to visualize bands. Excised bands were subjected to LC-MS/MS analysis as outlined below.

For co-immunoprecipitation analysis, primary murine keratinocytes transduced with pBabe-EGFP or pBabe-Psph-EGFP were lysed in 50 mM Tris-HCl, 150 mM NaCl, 1 mM EDTA, 1% NP40, 0.5% sodium deoxycholate, 0.1% SDS, 1 mM Na_3VO_4, 1mM PMSF, 1 μg/ml leupeptin and 1 μg/ml aprotinin and lysates were incubated with a GFP antibody (Abcam). Psph complexes were precipitated with Protein A sepharose and subjected to SDS-PAGE as outlined above.

2.7 LC-MS/MS analysis

Protein bands were subjected to in-gel digestion and peptide extracts were subjected to LC-MS/MS analysis on a Micromass Q-Tof hybrid quadrupole/time-of-flight mass spectrometer with a nanoelectrospray source. Capillary voltage was set at 1.8kV and cone voltage 32V; collision energy was set according to mass and charge of the ion, from 14eV to 50eV. Chromatography was performed on an LC Packings HPLC with a C18 PepMap column

using a linear acetonitrile gradient with flow rate of 200 nl/min. Raw data files were processed using the MassLynx ProteinLynx software and .pkl files were submitted for searching at www.matrixscience.com using the Mascot algorithm. Peptide data can be accessed by the following link: www.matrixscience.com/cgi/master_results.pl?file=../data/20101018/FteeifHOE.dat.

2.8 Tissue and cell immunolabeling

For immunohistochemical labeling of mouse tissue sections, purified 5B2 antibody was biotin-conjugated using EZ-Link Sulfo-NHS-LC-Biotin Kit as per manufacturer instruction (Pierce). Six μm histological sections of paraffin-embedded murine skin were probed with biotin-conjugated 5B2 antibody followed by detection with streptavidin-conjugated HRP using DAB (BioGenex) as a chromagen. Six μm cryosections of human skin and SCCs were stained with purified 5B2 antibody and Krt14 antibodies (Covance) followed by detection with anti-mouse Alexa Fluor-conjugated secondary antibodies (Invitrogen). Fluorescent and bright field images were captured on a Zeiss Axioplan 2 microscope.

Cultured cells were fixed in 4% pfa, permeabilized in 0.3% triton and stained with 5B2, Krt14 (Covance), Ki67 (Abcam), Calreticulin (Abcam), TGN38 (Abcam), or Lamp1 (DSHB) antibodies; or Lysotracker Green (Invitrogen) or Mitotracker Green (Invitrogen) organelle probes. Unconjugated primary antibodies were detected using species-specific Alexa Fluor-conjugated secondary antibodies (Invitrogen). Fluorescent images were captured on a Zeiss Inverted Axiovert 200M spinning disc confocal microscope.

2.10 Mutagenesis and phosphatase assay

Insertional mutagenesis of Psph Asp^{20} to Asn^{20} was conducted by PCR using *Pfu* DNA polymerase (Stratagene) and oligonucleotide primers, 5′-CGGATGCAGTGTGCTTTAATGTTGATAGCACCGT-3′ (sense) and 5′-ACGGTGCTATCAACATTAAAGCACACTGCATCCG-3′ (anti-sense), on murine Psph cDNA and confirmed by sequencing analysis (data not shown). Wt Psph and $Psph^{Asn20}$ subcloned into the pETGEXCT GST vector for production of recombinant Psph-GST and $Psph^{Asn20}$-GST fusion proteins in BL21 (DE3) pLysE cells (Invitrogen), which were purified using the MagneGST purification kit (Promega). Phosphatase assays were conducted on GST, Psph-GST or $Psph^{Asn20}$-GST recombinant proteins using a para-nitrophenyl phosphate (pNPP) Phosphatase Assay Kit as per manufacturer instruction (BioAssay Systems). The production of *p*-nitrophenol was measured by spectrophotometry at 405 nm and used to calculate phosphatase enzyme activity (Beer-Lambert). Phosphatase activities (μmoles/min/μg) were statistically compared between GST, Psph-GST or $Psph^{Asn20}$-GST recombinant proteins using a Student's t-Test.

2.9 Isolation of Nuclear and Cytoplasmic Cell Fractions

Nuclear and cytoplasmic fractions were isolated from primary mouse keratinocytes transduced with pBabe-EV, pBabe-EGFP or pBabe-Psph-EGFP retroviral vectors using the Nuclear Extract Kit according to manufacturer instruction (Active Motif). Fractions were subjected to SDS-PAGE followed by immunoblotting as outlined above.

2.11 Annexin V analysis

Murine keratinocytes transduced with pBabe-EGFP, pBabe-Psph-EGFP or pBabe-$Psph^{Asn20}$-EGFP retroviral vectors were stained for Annexin V (Cell Lab ApoScreen Annexin V-PE Apoptosis kit) as per manufacturer instruction (Beckman Coulter). The percentage of Annexin V^+ cells in each group was detected by FACS analysis performed on a LSRII FACS scanner (BD Biosciences). Data were analyzed using the FlowJo Flow

Cytometry Analysis software (Tree Star). The average percentage of DAPI-negative Annexin V^+ cells was compared between pBabe-EGFP, pBabe-Psph-EGFP and pBabe-$Psph^{Asn20}$-EGFP transduced cells (n = 3 replicates/group).

3. Results

3.1 Expression of Psph in mouse skin

We previously identified Psph by RNA microarray analysis to be highly induced in α6β4 integrin transgenic mouse epidermis compared to Wt epidermis in response to tumor promoter treatment. We confirmed these earlier findings by conducting RT-PCR analysis for Psph in RNA isolated from TPA- and vehicle-treated α6β4 integrin transgenic and Wt mouse epidermis (Fig. 1a). α6β4 integrin transgenic mice are highly sensitive to chemically induced skin SCC formation due to excessive epidermal proliferation in response to TPA tumor promotion [13]. Psph levels were elevated 2–3 fold in α6β4 integrin transgenic compared to Wt skin (Fig. 1a) suggesting a role for Psph in skin proliferation and/or tumorigenesis.

To begin to determine a role for Psph in skin homeostasis we generated monoclonal antibodies against murine Psph. Murine and human Psph homologs are both 225 amino acid proteins with a predicted molecular weight of 25 kD. Purified supernatant from Psph murine hybridoma clone 5B2 recognized an apparent 25 kD protein in both mouse and human keratinocytes (Fig. 1b) and an approximate 52 kD protein in cells transduced with the pBabe retroviral vector encoding a Psph-EGFP fusion protein (Fig. 1b). A single 25 kD was also detected in lysates derived from mouse liver and lung, tissues reported to exhibit strong Psph expression, at markedly higher levels compared to mouse epidermis (Fig. 1c). Low levels of Psph were also detected in mouse brain lysate upon longer film exposure (data not shown). Collectively, these results confirm that Psph is the major protein recognized by the 5B2 antibody by immunoblot analysis. In murine skin, strong immunodetection of Psph was localized in the cytoplasm of keratinocytes in the proliferative epithelial layer of the epidermis, hair follicles and sebaceous glands (Fig. 1d–e) and Psph expression was also detected in the differentiated layers of the epidermis (Fig. 1d–e). An analogous pattern of expression for Psph was also detected in normal human skin where strong Psph immunolabeling was observed in the Krt14-expressing basal epidermal layer (Fig. 1f–h). To further confirm the status of Psph in epidermal keratinocytes, primary cultures of murine keratinocytes were labeled with the 5B2 antibody in conjunction with either Krt14 (keratinocyte marker) or Ki67 (proliferation marker) antibodies. Strong Psph immunolabeling was localized primarily in the cytoplasm of $Krt14^+$ (Fig. 1i–k) and in $Ki67^+$ (Fig. 1l–n) mouse keratinocytes. Interestingly, the distribution of Psph immunolabeling in mouse keratinocytes suggests that Psph may be primarily localized to cellular organelles (Fig. 1i). These results indicate that Psph is an approximate 25 kD protein that is strongly expressed in epithelial keratinocytes of mammalian skin.

3.2 Psph localizes to late endosomes in mouse keratinocytes

To further characterize Psph, we investigated its sub-cellular localization in primary cultures of epidermal keratinocytes. Consistent with its expression pattern in skin tissue (Fig. 1), Psph was largely localized in the cytoplasm of primary keratinocytes and was concentrated to the perinuclear region in a staining pattern that was consistent with organelle distribution (Fig. 2a–f). Co-labeling studies with a panel of markers for sub-cellular organelles showed that Psph primarily associated with Lamp1+ late endosomes (Fig. 2r) and did localize to lysosomes (Fig. 2n), the nuclear membrane (Fig. 2o), mitochondria (Fig. 2p) or trans-Golgi (Fig. 2q); however, we cannot rule out a small fraction of Psph protein associating with the endoplasmic reticulum (Fig. 2m). A similar staining patter for Psph was observed in primary

cultures of human keratinocytes (data not shown). To confirm the cytoplasmic immunolocalization of Psph in keratinocytes, cytoplasmic and nuclear fractions were isolated from mouse keratinocytes transduced with an empty pBabe, pBabe-EGFP or pBabe-Psph-EGFP retrovector. The Psph-EGFP fusion protein was detected by immunoblot analysis in cytoplasmic fractions of keratinocytes but not in the nuclear fraction (Fig. 3a). In addition, endogenous Psph protein was also absent in nuclear lysates generated from normal human liver and Rb-expressing lung tissues (Fig. 3b).

3.3 PSPH functions as a homodimer

Homodimerization is a conserved feature of HAD proteins [19], prompting us to investigate whether PSPH may also exist in a dimeric form or interact with other proteins outside of canonical L-serine biosynthesis. To determine this, we employed a tandem affinity purification approach using a HA- and FLAG-tagged PSPH protein as bait in HEK293 epithelial cells to identify potential PSPH interacting proteins. We observed a single candidate band by SDS-PAGE silver staining (Fig. 3c–d) that was subsequently identified by LC-MS/MS analysis to be human PSPH (data not shown) indicating that PSPH may exist in multimeric form. This possibility was confirmed by GFP immunoprecipitation in lysates from keratinocytes transduced with either pBabe-EGFP or pBabe-Psph-EGFP followed by Psph immunoblot analysis. Endogenous Psph was precipitated by GFP antibodies in pBabe-Psph-EGFP keratinocytes but not in pBabe-EGFP keratinocytes (Fig. 3e). Finally, immunoblot analysis under non-reducing conditions identified a single endogenous PSPH multimer of approximately 50 kD in HEK293 cells (Fig. 3f) indicating that PSPH is primarily present as a homodimer in epithelial cells. Similar results were obtained in multiple human epithelial cell lines (data not shown).

3.4 PSPH regulates keratinocyte proliferation

Our initial findings of induced Psph levels in hyperproliferative murine epidermis suggest that Psph may play a role in epithelial proliferation (Fig. 1). To explore this possibility further, we analyzed PSPH levels in huSCC13 and huSCC35 keratinocytes isolated under pre-confluent, highly proliferative conditions compared to confluent conditions where cells are largely contact inhibited. PSPH protein levels were approximately 5–7 fold higher in huSCC13 and huSCC35 cultures growing at 20–40% confluency compared to cultures at 80–100% confluency (Fig. 4a–b; data not shown). These results support the idea that PSPH is induced under proliferative conditions in epithelial cells but do not exclude the possibility that cell-cell contact may also suppress PSPH expression.

To further delineate the role of PSPH in keratinocyte proliferation, huSCC13 and huSCC35 keratinocyte cultures were transduced with the Dox-inducible pTRIPZ lentiviral vector encoding a short hairpin RNA targeting PSPH (shPSPH) or a non-silencing control (shNS). We typically observed 70–90% knockdown of PSPH protein in Dox-treated SCC keratinocytes transduced with shPSPH compared to untreated cells (Fig. 4c–d). PSPH levels were unaltered in shNS transduced SCC cells treated with Dox (Fig. 4c–d). To measure proliferation we subjected shPSPH and shNS SCC cells (huSCC13 and huSCC35) to clonogenic growth assays [13] in growth medium containing an excess of L-serine (3.25 mM) and either treated untreated with Dox. Colony forming efficiency was decreased approximately 4-fold in shPSPH huSCC13 cells and 2-fold in shPSPH huSCC35 cells compared to shNS huSCC13 and shNS huSCC35 cells, respectively (Fig. 4e–g). The dramatic reduction in proliferation in PSPH-deficient SCC keratinocytes observed under excessive L-serine conditions, suggests that new roles may exist for PSPH outside of L-serine biosynthesis that are critical for epithelial cell proliferation.

To begin to explore the molecular basis of L-serine-independent regulation of SCC proliferation by PSPH, we analyzed shPSPH and shNS huSCC13 cells for levels of the cell cycle regulator cyclin D1. We found cyclin D1 levels to be dramatically reduced in Dox-treated shPSPH but not shNS huSCC13 cells (Fig. 5a) suggesting that Psph may play a role in entry into the cell cycle. To exclude the possibility that the reduced colony numbers in shPSPH SCC cells may be due to increased apoptosis we also analyzed cleaved PARP levels in shPSPH huSCC13 cells compared to shNS huSCC13 cells. No differences in cleaved PARP levels were observed between shPSPH- and shNS-transduced huSCC13 cells (Fig. 5a) indicating that the decreased colony numbers in shPSPH-transduced huSCC13 and huSCC35 cells was not due to induction of apoptosis. We also confirmed that loss of Psph enzymatic phosphatase activity does not induce apoptosis in murine keratinocytes that overexpressed an EGFP-tagged phosphatase-deficient Psph mutant ($Psph^{Asn20}$-EGFP). The phosphatase-deficient mutant Psph was generated by replacing the first conserved aspartate (Asp^{20}) contained within the normal phosphatase motif DVDST with an asparagine (Asn^{20}) resulting in an inactive domain, NXDXT. Consistent with previous studies of Psph and other HAD family members [3–4], we found the first conserved aspartate to be most critical for the Psph phosphatase activity (Fig. 5b). Overexpression of Wt Psph or $Psph^{Asn20}$ did not increase the number of Annexin V+ cells as determined by FACS analysis (Fig. 5c). Collectively, these results exclude a role for PSPH in epithelial cell apoptosis and suggest that the presence of PSPH is critical for SCC proliferation in a L-serine biosynthesis-independent fashion.

3.5 PSPH is induced during skin carcinogenesis

To determine whether PSPH expression may be altered in skin carcinogenesis *in vivo*, we examined the levels and localization of PSPH in murine and human cutaneous skin tumors. Psph protein levels were upregulated in both benign papillomas and SCCs induced by a two-stage DMBA/TPA skin carcinogenesis protocol [14] compared to normal epidermis (Fig. 5d). Similarly, PSPH levels were also constitutively induced in human SCC keratinocytes compared to normal adult keratinocytes (Fig. 5e). Immunohistochemical labeling of histological tissue sections demonstrated that Psph was strongly expressed in epidermal keratinocytes within murine benign papillomas (Fig. 5f) and malignant SCC, including areas containing atypical cells (Fig. 5g), indicating that the high expression levels of Psph in murine skin tumors (Fig. 5d–e) are largely derived from neoplastic keratinocytes. Collectively, these results indicate that PSPH induction is an early and maintained event in cutaneous SCC pathogenesis.

4. Discussion

In this study, we provide evidence for a fundamental role for the HAD family enzyme PSPH in SCC proliferation. Typically, increased L-serine biosynthesis would support tumor cells by providing amino acid and nucleotide substrates necessary for cell division. Therefore, the induction of PSPH observed in proliferating keratinocytes in normal and neoplastic skin may in part be due to the requirement for the L-serine biosynthetic pathway. However, the marked reduction in SCC proliferation in PSPH knock down cells occurred in the presence of excess exogenous L-serine suggesting that additional roles for PSPH in the proliferation of neoplastic epithelial cells may exist outside of its role in L-serine biosynthesis. Overall these findings suggest that PSPH may have additional enzymatic substrates or novel non-enzymatic interacting proteins in epithelial cells that may be important for carcinogenesis.

Multiple lines of direct evidence show that HAD hydrolase family members can function outside of their canonical metabolic pathways and influence cell behavior and that the DXDXT catalytic motif can facilitate phosphate transfer on a variety of molecular substrates. For example, chronophin exhibits protein phosphatase activity on the actin-

depolymerizing factor cofilin, by dephosphorylating a single serine residue through its DXDXT motif, thereby implicating a role for chronophin in cell division, growth and motility [20]. The N-terminal domain of the epoxide hydrolase EPXH2 protein bears high homology to HAD proteins and has reported lipid phosphate phosphatase activity [21], and PHOSPHO1 is a HAD family protein with proven phosphatase activity on phosphoethanolamine and phosphocholine [22]. In addition emerging evidence shows that Psph levels are uniquely regulated in certain stem cell populations and suggests that PSPH may play a role in cell fate decisions. Psph levels are enriched in hematopoietic stem cells [23] and neural stem cells in mouse [23–25]. The *Drosophila* homolog of PSPH, *aay*, a can be induced by Ras in proliferative hemocytes [26] and is also involved in neuronal cell fate determination [27].

Some attractive possibilities for PSPH functions outside of L-serine metabolism include protein or lipid phosphorylation or modulation of cell signaling pathways by non-enzymatic means. While our initial immunoprecipitation studies did identify PSPH as a homodimer, we did not identify novel phosphoprotein substrates or additional interacting proteins. Although our cell proliferation studies were conducted in excess L-serine conditions, we cannot conclusively rule out the possibility that loss of PSPH may still perturb the L-serine biosynthetic pathway and lead to aberrant production of metabolic intermediates and diminished cell proliferation. Whether phospholipid or other non-enzymatic substrates exist for PSPH that can influence cell proliferation will be the subject of future studies. In addition, it will also be critical to determine whether the influence of PSPH on SCC proliferation observed in tissue culture is maintained *in vivo* under natural carcinogenesis conditions.

In summary, we identified the HAD family protein PSPH to be expressed in the epidermis of mammalian skin and highly induced in skin tumors. PSPH appears to be critical for the proliferation of SCC cells; however, it is unclear whether this phenomenon may due to non-enzymatic activity or phosphatase activity on other cellular substrates besides phosphoserine. In as much, these studies show that PSPH may serve as novel therapeutic target to modulate cutaneous SCC, and our future work will focus on profiling human SCC signaling pathways that are important for proliferation and are also compromised as a consequence of blocking PSPH expression.

Acknowledgments

We thank Mary Ann Gawinowicz (HICCC Proteomics Core Facility) for technical assistance. Lentiviral packaging (psPAX2) and envelope (pMD2.G) plasmids were generated in the laboratory of Didier Trono. We thank David Bickers and Angela Christiano for providing HEK293 and 293T cells, respectively. This work was supported by NIH R03AR054071 (DMO) and F32AR055007 (MAB) research grants.

References

1. Borkenhagen LF, Kennedy EP. The enzymic equilibration of L-serine with O-phospho-L-serine. Biochim Biophys Acta. 1958; 28:222–223. [PubMed: 13535713]
2. Neuhaus FC, Byrne WL. O-Phosphoserine phosphatase. Biochim Biophys Acta. 1958; 28:223–224. [PubMed: 13535714]
3. Collet JF, Gerin I, Rider MH, Veiga-da-Cunha M, Van Schaftingen E. Human L-3-phosphoserine phosphatase: sequence, expression and evidence for a phosphoenzyme intermediate. FEBS Lett. 1997; 411:251–254. [PubMed: 9271215]
4. Collet JF, Stroobant V, Pirard M, Delpierre G, Van Schaftingen E. A new class of phosphotransferases phosphorylated on an aspartate residue in an amino-terminal DXDX(T/V) motif. J Biol Chem. 1998; 273:14107–14112. [PubMed: 9603909]

5. Collet JF, Stroobant V, Van Schaftingen E. Mechanistic studies of phosphoserine phosphatase, an enzyme related to P-type ATPases. J Biol Chem. 1999; 274:33985–33990. [PubMed: 10567362]
6. de Koning TJ, Snell K, Duran M, Berger R, Poll-The BT, Surtees R. L-serine in disease and development. Biochem J. 2003; 371:653–661. [PubMed: 12534373]
7. Tabatabaie L, Klomp LW, Berger R, de Koning TJ. L-serine synthesis in the central nervous system: A review on serine deficiency disorders. Mol Gen Metab. 2010; 99:256–262.
8. Pollari S, Kakonen SM, Edgren H, Wolf M, Kohonen P, Sara H, Guise T, Nees M, Kallioniemi O. Enhanced serine production by bone metastatic breast cancer cells stimulates osteoclastogenesis. Breast Cancer Res Treat. 2011; 125:421–430. [PubMed: 20352489]
9. Tan EH, Ramlau R, Pluzanska A, Kuo HP, Reck M, Milanowski J, Au JS, Felip E, Yang PC, Damyanov D, Orlov S, Akimov M, Delmar P, Essioux L, Hillenbach C, Klughammer B, McLoughlin P, Baselga J. A multicentre phase II gene expression profiling study of putative relationships between tumour biomarkers and clinical response with erlontinib in non-small-cell lung cancer. Ann Oncol. 2010; 21:217–222. [PubMed: 20110292]
10. Greengard O, Head JF, Chahinian AP, Goldberg SL. Enzyme pathology of human mesotheliomas. J Natl Cancer Inst. 1987; 78:617–622. [PubMed: 2882044]
11. Shimomura K, Sakakura C, Takemura M, Takagi T, Fukuda K, Kin S, Nakase Y, Miyagawa K, Ohgaki M, Fujiyama J, Fujita Y, Nakanishi M, Hagiwara A, Shirane M, Okazaki Y, Hayashizaki Y, Yamagishi H. Combination of L-3-phosphoserine phosphatase and CEA using real-time RT-PCR improves accuracy in detection of peritoneal micrometastasis of gastric cancer. Anticancer Res. 2004; 24:1113–1120. [PubMed: 15154633]
12. Hemmati HD, Nakano I, Lazareff JA, Masterman-Smith M, Geschwind DH, Bronner-Fraser M, Kornblum HI. Cancerous stem cells can arise from pediatric brain tumors. Proc Natl Acad Sci USA. 2003; 100:15178–15183. [PubMed: 14645703]
13. Owens DM, Romero RM, Gardner C, Watt FM. Suprabasal α6β4 integrin expression in epidermis results in enhanced tumorigenesis and disruption of TGFβ signaling. J Cell Sci. 2003; 116:3783–3791. [PubMed: 12902406]
14. Stumpfova M, Ratner D, Desciak EB, Eliezri YD, Owens DM. The immunosuppressive surface ligand CD200 augments the metastatic capacity of squamous cell carcinoma. Cancer Res. 2010; 70:2962–2972. [PubMed: 20332223]
15. Jensen UB, Yan X, Triel C, Woo SH, Christensen R, Owens DM. A distinct population of clonogenic and multipotent murine follicular keratinocytes residing in the upper isthmus. J Cell Sci. 2008; 121:609–617. [PubMed: 18252795]
16. Rheinwald JG, Green H. Serial cultivation of strains of human epidermal keratinocytes: the formation of keratinizing colonies from single cells. Cell. 1975; 6:317–330. [PubMed: 1052770]
17. Morgenstern JP, Land H. Advanced mammalian gene transfer: high titre retroviral vectors with multiple drug selection markers and a complementary helper-free packaging cell line. Nucleic Acids Res. 1990; 18:3587–3596. [PubMed: 2194165]
18. Levy L, Broad S, Zhu AJ, Carroll JM, Khazaal I, Peault B, Watt FM. Optimised retroviral infection of human epidermal keratinocytes: long-term expression of transduced integrin gene following grafting on to SCID mice. Gene Ther. 1998; 5:913–922. [PubMed: 9813662]
19. Kurihara T, Esaki N. Bacterial hydrolytic dehalogenases and related enzymes: occurrences, reaction mechanisms, and applications. Chem Rec. 2008; 8:67–74. [PubMed: 18366103]
20. Gohla A, Birkenfeld J, Bokoch GM. Chronophin, a novel HAD-type serine protein phosphatase, regulates cofilin-dependent actin dynamics. Nat Cell Biol. 2005; 7:21–29. [PubMed: 15580268]
21. Newman JW, Morisseau C, Harris TR, Hammock BD. The soluble epoxide hydrolase encoded by EPXH2 is a bifunctional enzyme with novel lipid phosphate phosphatase activity. Proc Natl Acad Sci USA. 2003; 100:1558–1563. [PubMed: 12574510]
22. Roberts SJ, Stewart AJ, Sadler PJ, Farquharson C. Human PHOSPHO1 exhibits high specific phosphoethanolamine and phosphocholine phosphatase activities. Biochem J. 2004; 382:59–65. [PubMed: 15175005]
23. Terskikh AV, Easterday MC, Li L, Hood L, Kornblum HI, Geschwind DH, Weissman IL. From hematopoiesis to neuropoiesis: evidence of overlapping genetic programs. Proc Natl Acad Sci. 2001; 98:7934–7939. [PubMed: 11438738]

24. Geschwind DH, Ou J, Easterday MC, Dougherty JD, Jackson RL, Chen Z, Antoine H, Terskikh A, Weissman IL, Nelson SF, Kornblum HI. A genetic analysis of neural progenitor differentiation. Neuron. 2001; 29:325–339. [PubMed: 11239426]

25. Nakano I, Dougherty JD, Kim K, Klement I, Geschwind DH, Kornblum HI. Phosphoserine phosphatase is expressed in the neural stem cell niche and regulates neural stem and progenitor cell proliferation. Stem Cells. 2007; 25:1975–1984. [PubMed: 17495110]

26. Asha H, Nagy I, Kovacs G, Stetson D, Ando I, Dearolf CR. Analysis of Ras-induced overproliferation in Drosophila Hemocytes. Genetics. 2003; 163:203–215. [PubMed: 12586708]

27. Egger B, Leemans R, Loop T, Kammermeier L, Fan Y, Radimerski T, Strahm MC, Certa U, Reichert H. Gliogenesis in Drosophila: genome-wide analysis of downstream genes of glial cells missing in the embryonic nervous system. Development. 2002; 129:3295–3309. [PubMed: 12091301]

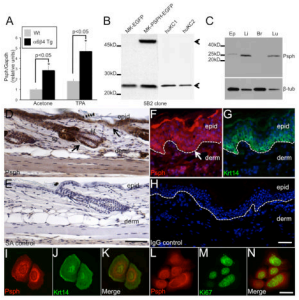

Fig. 1.

PSPH is expressed in the epidermis of murine and human skin.

A. Bar graph depicting relative Psph levels quantified by RT-PCR analysis on epidermal RNA samples isolated from acetone- and TPA-treated Wt and α6β4 transgenic mouse skin. Psph levels are normalized by expression of Gapdh. B. Immunoblot validation of monoclonal Psph antibody 5B2 in primary murine, MK-EGFP and MK-Psph-EGFP, and human, huKC1 and huKC2, keratinocyte cultures. Arrow points to an apparent 25 kD protein in all cells (PSPH; lower) or 52 kD fusion protein (PSPH-EGFP; upper) only observed in MK-PSPH-EGFP cells. C. Immunoblot detection of Psph in lysates generated from murine epidermis (Ep), liver (Li), brain (Br), and lung (Lu) tissues. Tubulin (lower panel) levels were assessed to confirm protein loading. D–H. Immunohistochemical detection of Psph in adult murine skin (DAB staining) (D) and immunofluorescent co-labeling of PSPH (F) and Krt14 (G) in human foreskin. No labeling was observed in streptavidin (E) or IgG (H) control-stained sections. Arrows point to strong Psph labeling in the basal layer of the epidermis (D, F). Panels F–G represent the same field of view. I–N. Immunofluorescent co-labeling of Psph and Krt14 (I–K) or Psph and Ki67 (L–N) in primary murine keratinocyte cultures. Panels I–K and L–N represent the same field of view. Abbreviations: epid, epidermis; derm, dermis; sg, sebaceous gland; hf, hair follicle; SA, streptavidin; Wt, wild-type. Scale bar: 50 μm (DE); 20 μm (F–H); 10 μm (I–N).

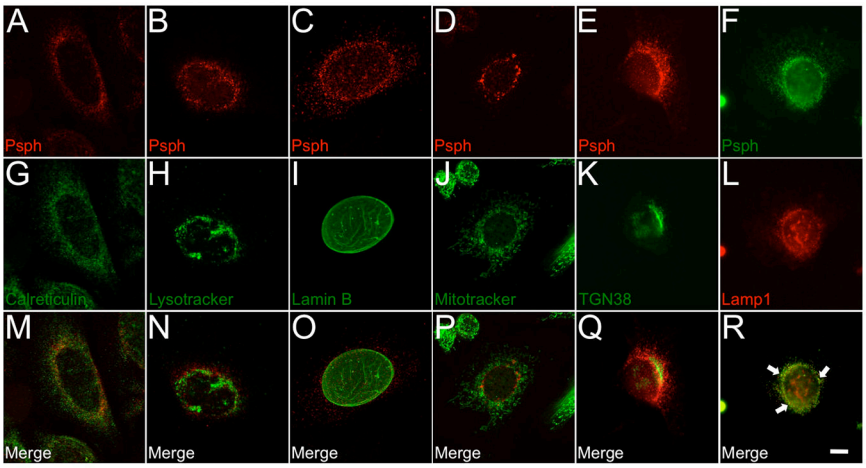

Fig. 2.

Sub-cellular localization of Psph in mouse keratinocytes.

A–F. Primary mouse keratinocytes were co-labeled with Psph monoclonal antibody 5B2 and markers for the following sub-cellular structures: endoplasmic reticulum (G), lysosomes (H), nuclear membrane (I), mitochondria (J), trans-Golgi (K) and endosomes (L). M–R. Merged panels for each co-labeled group were generated to confirm the localization of Psph. Scale bar: 10 μm.

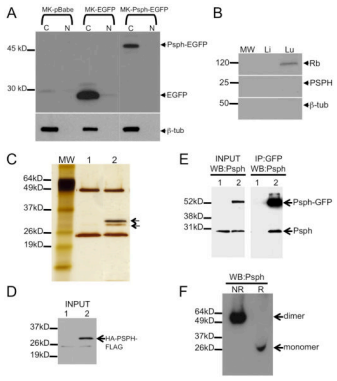

Fig. 3.

Cytoplasmic Psph functions as a homodimer.

A. GFP immunoblot analysis of cytosolic (C) and nuclear (N) lysates from murine keratinocytes (MK) transduced with pBabe-EV, pBabe-EGFP or pBabe-Psph-EGFP retroviral vectors. Arrows point to 52 kD Psph-EGFP fusion protein (upper) or EGFP (lower). Lower blot shows immunodetection of tubulin only in cytosolic lysates of each group. B. Rb (top), PSPH (middle) and tubulin (bottom) immunoblot analysis of nuclear lysates derived from human liver (Li) and lung (Lu) tissue. C. Silver-stained acrylamide gel of anti-HA and anti-FLAG tandem affinity purification in HEK293 cells transfected with pcDNA3 empty vector (1) or pcDNA3-HA-PSPH-FLAG vector (2). Bands marked with arrows were identified by LC-MS/MS to be HA-PSPH-FLAG (upper) and endogenous PSPH (lower). D. Immunoblot analysis showing detection of input levels of HA-PSPH-FLAG expression (arrow) in pcDNA3-HA-PSPH-FLAG transfected (2) but not in pcDNA3 empty vector transfected (1) cells used above in A. E. Psph immunoblot analysis of lysates from primary keratinocytes overexpressing EGFP (1) or Psph-EGFP fusion protein (2) either input (left panel) or immunoprecipitated with EGFP antibodies (right panel). Arrows point to detection of the Psph-EGFP fusion protein (upper) or endogenous Psph (lower). F. Psph immunoblot analysis of whole cell lysates from HEK293 cells subjected to PAGE under non-reducing (NR) and reducing (R) conditions. Abbreviations: MW, molecular weight ladder.

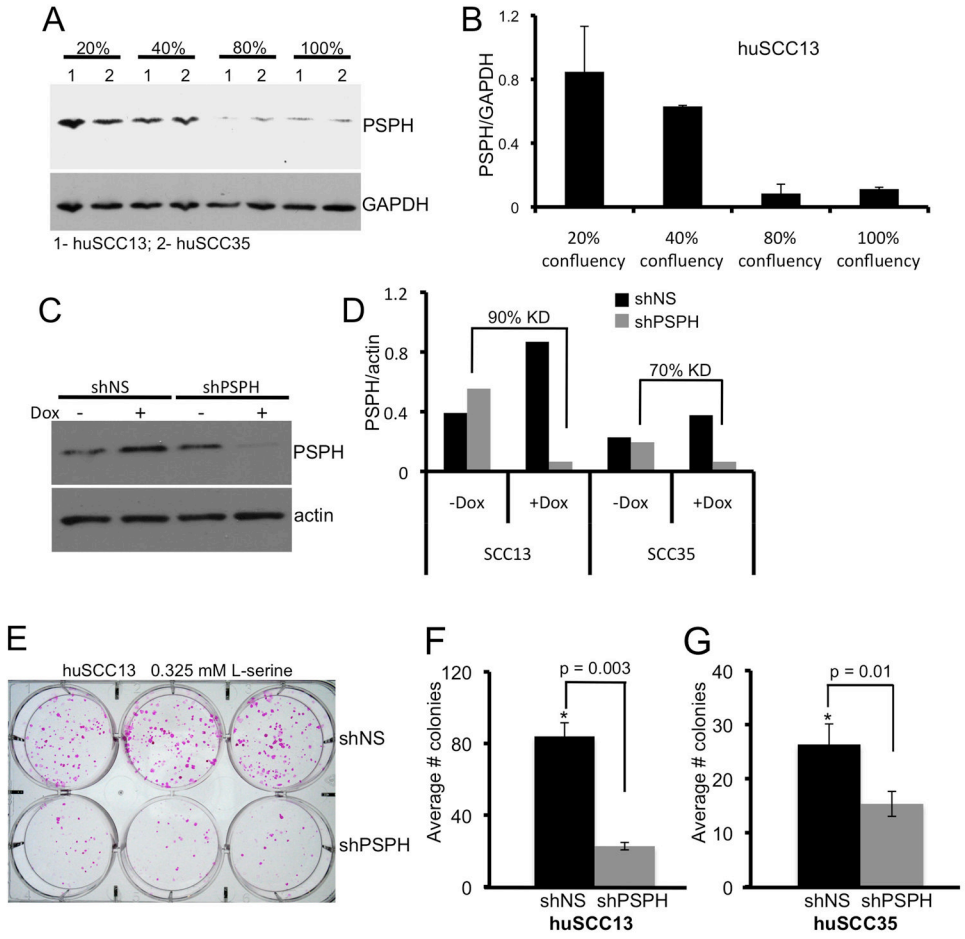

Fig. 4.

Effect of PSPH on keratinocyte proliferation.

A. PSPH immunoblot analysis in pre-confluent (20–40%) and confluent (80–100%) cultures of huSCC13 (1) and huSCC35 (2) cells. GAPDH immunoblot indicates protein loading. B. Bar graph depicting relative densitometric units of Psph protein levels normalized to GAPDH levels (from A) in pre-confluent and confluent huSCC13 keratinocyte cultures. Error bars represent the average of duplicate experiments. C. Psph immunoblot analysis showing knock down of PSPH in human SCC keratinocytes transduced with a Dox-inducible shRNA targeting PSPH (shPSPH) or a non-silencing control (shNS). Actin (lower panel) levels were assessed to confirm protein loading. D. Bar graph depicting relative densitometric units of Psph protein levels normalized to actin levels (from C) in shNS and shPSPH transduced human huSCC13 and huSCC35 (immunoblot not shown) keratinocyte cultures treated or untreated with Dox. E. Colony forming assay showing Rhodamine A-stained cultures of shNS and shPSPH huSCC13 keratinocytes cultured for 14 days with Dox. F. Bar graph depicting the quantification of colonies > 4 mm in size in shNS and shPSPH transduced huSCC13 cells. Error bars represent the standard deviation of three replicate plates. G. Bar graph depicting the quantification of colonies > 4 mm in size in shNS and shPSPH transduced huSCC35 cells (colony assay plates not shown). Error bars represent the standard deviation of three replicate plates.

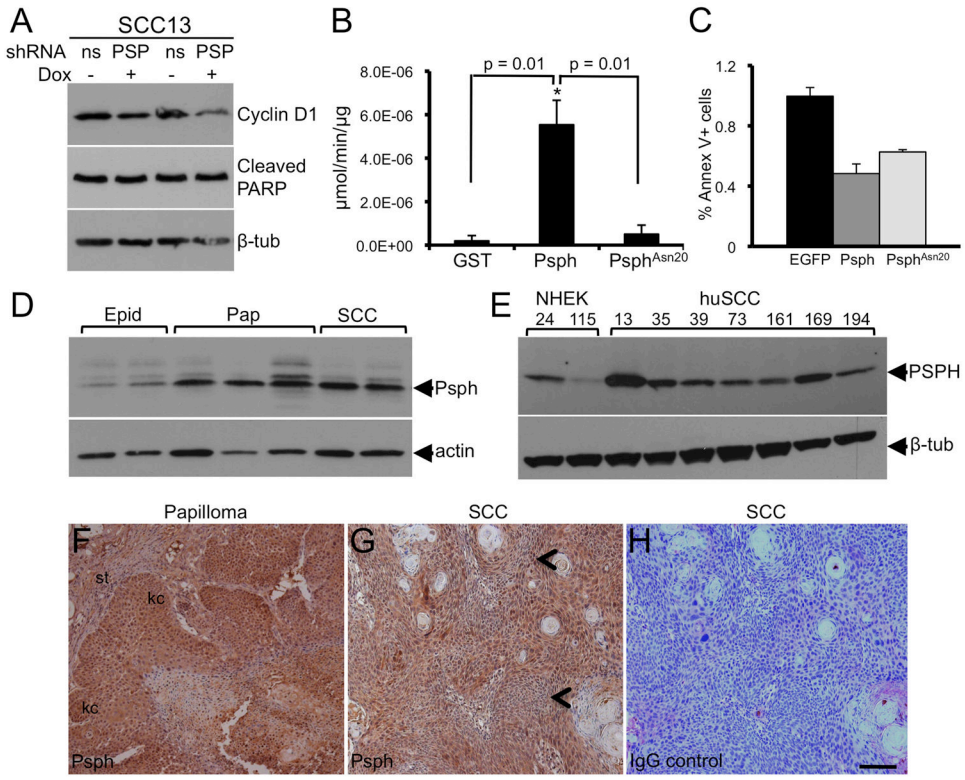

Fig. 5.

PSPH is induced in murine and human skin tumors.

A. Cyclin D1 and cleaved PARP immunoblot analysis in shNS and shPSPH huSCC13 keratinocytes treated (+) or untreated (−) with Dox. Tubulin (lower panel) levels were assessed to confirm protein loading. B. Bar graph depicting enzymatic phosphatase activity on para-nitrophenyl-phosphate by recombinant GST, Psph-GST or Psph^{Asn20}-GST proteins. Error bars represent the standard deviation of three replicate assays. C. Bar graph depicting the percentage of Annexin V+ cells as determined by FACS analysis in murine keratinocytes transduced with pBabe-EGFP, pBabe-Psph-EGFP or pBabe-Psph^{Asn20}-EGFP retroviral vectors. Error bars represent the standard deviation of three replicate assays. D. PSPH immunoblot analysis of whole cell lysates from normal murine epidermis (Epid), benign papillomas (Pap) and SCCs. E. PSPH immunoblot analysis of lysates derived from 2 separate cultures (PK24, PK115) of primary normal and 7 separate cultures (huSCC13, huSCC35, huSCC39, huSCC73, huSCC161, huSCC169, huSCC194) of SCC human keratinocytes. Actin (D) or tubulin (E) levels were assessed to indicate protein loading. F–H. Immunolocalization of Psph in murine papilloma (F) and cutaneous SCC (G) tissue sections. Arrow heads point to areas containing atypical cells in G. Panel H represents a secondary antibody-stained control serial section of panel G. Abbreviations: kc, keratinocytes; st, stroma. Scale bar: 50 μm.